Received: 23 June 2019 | Revised: 4 March 2020 | Accepted: 25 March 2020

DOI: 10.1111/jfpp.14477



ORIGINAL ARTICLE

Journal of Food Processing and Preservation | Institute of Food Science + Technology | ifst | WILEY

# Quality properties and mathematical modeling of vinasse films obtained under different conditions

Lionel Cortes[1] | Mario Pérez-Won[2] | Roberto Lemus-Mondaca[3] | Claudia Giovagnoli-Vicuna[1] | Elsa Uribe[1,4]

[1]Departamento de Ingeniería en Alimentos, Universidad de La Serena, La Serena, Chile

[2]Departamento de Ingeniería en Alimentos, Universidad del Bío-Bío, Chillán, Chile

[3]Departamento de Ciencia de los Alimentos y Tecnología Química, Facultad de Ciencias Químicas y Farmacéuticas, Universidad de Chile, Independencia, Santiago, Chile

[4]Instituto de Investigación Multidisciplinario en Ciencia y Tecnología, Universidad de La Serena, La Serena, Chile

**Correspondence**
Roberto Lemus-Mondaca, Departamento de Ciencia de los Alimentos y Tecnología Química, Facultad de Ciencias Químicas y Farmacéuticas, Universidad de Chile, Santos Dumont 964, Independencia, Santiago, Chile.
Email: rlemus@uchile.cl

**Funding information**
Departamento de Ingeniería en Alimentos, Universidad de La Serena, Grant/Award Number: PR16331 and PEQ16334; Compañía Pisquera de Chile

## Abstract

Vinasse (pisco distillation waste) is a promising feedstock for developing new high value-added bioproducts because it is supporting sustainable production as an agroindustrial by-product. The aims of this study were to evaluate experimental drying curves (60°C and 80°C); mathematical modeling of films and the effect of the drying conditions on quality properties of vinasse films plasticized with glycerol at different pH. The results indicated that as the drying temperature increased, the moisture ratio decreased for all films. The Weibull model obtained the best-fit quality of experimental results. The effective moisture diffusivity varied between 2.234 and 2.513 × $10^{-11}$ $m^2$/s. The optimal conditions were found at 80°C and pH 11 for films. Under these conditions, the films presented a higher tensile strength (26.54 MPa), lower elongation at break (6.82%), and a higher Young´s Modulus (385.32 MPa). Thus, vinasse films could be used as packaging or coating materials in the food industry.

## Practical applications

Currently, one of the most relevant challenges is the valorization of agroindustrial wastes, since promoting the sustainability and bioconversion of agro-industrial residues. In the case of the winery, this produces high amounts of wastes per annum in the different processes of production. These wastes can represent important environmental problems caused by their composition and organic burden. Therefore, the agro-industrial liquid residue generated in the distillation step from wine for pisco elaboration in Chile can be to able an opportunity for the valorization of this waste as biofilms or coatings.

## 1 | INTRODUCTION

One the most significant agricultural activities, in the world, is wine production. The European (Italy, Spain, France, Germany, and Portugal) and American (USA, Argentina, and Chile) countries are the most important contributors wine-producing zones of the world (Barba, Zhu, Koubaa, Anderson, Sant'Ana, & Orlien, 2016). Approximately 275.7 million hL (hectoliters) of wine are produced by these countries and about 13 million tons correspond to the residue of the wine-making process, which are usually used as fertilizer or discarded (Botelho, Bennemann, Torres, & Sato, 2018).

Vinasse is the liquid industrial residue generated in the distillation step from wine for *pisco* elaboration in Chile. The alcohol contained in the wine evaporates and then condenses; the remaining liquid is called as "*pisco distillation waste*." This residue is taken to the bottom of the still representing approximately 70%–75% volume of distilled wine (Callejas, Silva, Peppi, & Seguel, 2014). The waste has been a subject of research due to its content of antioxidant compounds that

  

can have relevant biological properties such as antioxidant and antibacterial activities (Bekhit et al., 2019). The antioxidant compounds are associated with different phenolic groups including phenolic acids, flavonoids, and stilbenes (Teixeira et al., 2014).

Edible films are a potential option for plastics in the food industry, which could reduce the use of plastic and avoid the impact on the environment (Daza, Homez-Jara, Solanilla, & Váquiro, 2018). However, plasticizer type, compound concentrations, drying temperature, source, and chemical structure of polymer are factors affecting the properties and structure of film during its preparation as the edible film (Homez-Jara et al., 2018). The drying temperature is one of the most important factors in the preparation of edible films because they establish reorganization or crystallinity of film as well as the mechanical, optical, and barrier properties of them (Daza et al., 2018). Several investigations have reported about different drying temperatures of edible films, for example, chitosan films were dried for 2 weeks at 2°C, for 1 week at 25°C and for 24 hr at 40°C (Homez-Jara et al., 2018); gelatin films at 25°C and 50°C for 24 hr (Chuaynukul et al., 2018) and, Na-alginate films at 15°C, 57°C and 90°C (Bagheri, Radi, & Amiri, 2019) and quality and barrier properties were determined.

Considering the potential industrial use of the waste from winemaking process, the aims of the present study were (a) to evaluate experimental drying curves (60°C and 80°C) and a mathematical modeling of vinasse films and (b) to the assessment the effect of the drying conditions on the thickness, moisture content, water activity, Attenuated Total Reflection Fourier Transform Infrared (ATR-FTIR) spectroscopy and texture from vinasse films plasticized with glycerol or sorbitol at different pH.

## 2 | MATERIALS AND METHODS

### 2.1 | Raw material characterization

Vinasse (organic) was provided by Compañía Pisquera de Chile S.A. (CPCh), located in Ovalle city, Region of Coquimbo, Chile, which was stored at 4.0°C ± 1.0°C until the moment of the experiment. The moisture content was determined employing a vacuum oven (OVL570, Gallenkamp) and an analytical accurate balance to ±0.0001 g (Jex120, CHYO). The crude protein content was determined using the Kjeldahl method (Nx6.25). The lipid content was analyzed gravimetrically following Soxhlet extraction. Crude ash was estimated by incineration in a muffle furnace (360D, Felisa) at 550°C. The crude fiber content was estimated by the Weende method through an acid/alkaline hydrolysis of insoluble residues as described in AOAC method No. 962.09. All methodologies followed the recommendations of the Official Method of Analysis (AOAC, 1990). All reagents were analytical grade. Glycerol (purity ≥ 99.5%), maltodextrin (DE = 16.0–19.5), Collagen (beef tissue, food grade), sorbitol, and sodium hydroxide (NaOH) were purchased from Sigma-Aldrich. All solutions were prepared using deionized water.

### 2.2 | Preparation and formation of the film

Twenty grams of vinasse was concentrated to 67 °Brix in a rotary evaporator (Büchi, R-210) under reduced pressure at 70°C, followed by the addition of the 5g glycerol and 15g collagen solution (on water in a 2:1 ratio (w/w)). Then, maltodextrin was added at 15% (w/w). All ingredients were homogenized in a rotor-stator homogenizer Ultra-turrax (IKA, T25) at 500 × *g* for 15min to room temperature (20°C). The homogenized was separated into two mixtures and the pH was regulated to 7.0 and 11.0 with NaOH (50% (w/v)), respectively. Immediately, 2.0g of the film-forming solution was gently transferred by pouring it into a glass Petri plate (100×15mm), in order to obtain a uniform initial thickness of the different poured solutions, resulting in an initial thickness of 0.6mm approximately. Then, film-forming solutions were dried by a heating oven with natural convection (Memmert, UF 110) and controlled temperature, in order to obtain vinasse films. The solutions weight was measured on an analytical balance (SP402, Ohaus) with an accuracy of ±0.01g at time defined, connected by a system interface (RS232, Ohaus) to a computer, which recorded and stored the weight decrease data. The experiments finished when reaching constant weight (i.e., equilibrium condition). Drying processes were carried out at 60°C and 80°C, in triplicate.

### 2.3 | Thin-layer drying model

The drying curves were obtained by plotting the moisture ratio (MR) versus time. The MR by the following equation (Moreira et al., 2011):

$$MR = \frac{M_t - M_e}{M_o - M_e} \quad (1)$$

where $M_t$ is the moisture content at any time $t$, $M_o$ is the initial moisture content, and $M_e$ is the equilibrium moisture content (kg water/kg dry matter). The equilibrium moisture content of vinasse films was obtained from the final moisture content of the drying process until samples reached a constant weight.

To fit the experimental data of the drying process, three thin-layer drying mathematical models were used (Zhou, Huang, Deng, & Xiao, 2018; Zura-Bravo, Rodriguez, Stucken, & Vega-Gálvez, 2019), which are given in Table 1.

**TABLE 1** Mathematical equations for fitting the experimental drying curves

| Model name | Equation | No. |
|---|---|---|
| Weibull | $MR = e^{(-(t/\beta)^{\alpha})}$ | (2) |
| Page | $MR = e^{-kt^n}$ | (3) |
| Modified page | $MR = e^{-(kt)^n}$ | (4) |

*Note:* Where $\alpha$ is the shape parameters and $\beta$ is the scale parameter of the Weibull model, while $n$ and $k$ are the empirical and kinetics parameters of Page and modified Page models. The MR (dependent variable) was obtained using the Equation (1).

The sum squared error ($R^2$, Equation 5) and Chi-square ($\chi^2$, Equation 6) statistical were used to evaluate fit quality between experimental and predicted data.

$$SSE = \frac{1}{N}\sum_{i=1}^{N}\left(\overline{MR}_{p,i} - MR_{e,i}\right)^2 \quad (5)$$

$$\chi^2 = \frac{\sum_{i=1}^{N}\left(MR_{p,i} - MR_{e,i}\right)^2}{N-z} \quad (6)$$

where $MR_{e,i}$ and $MR_{p,i}$ are experimental and predicted moisture ratio, respectively; $N$ is the number of observations and $z$ is the number of constants.

## 2.4 | Determination of the effective moisture diffusivity

The experimental data of the drying process were used for diffusivity coefficients determination by the Fick's second diffusion equation.

$$\frac{\partial M}{\partial t} = D_{eff}\nabla^2 M \quad (7)$$

Fick's second equation (Equation 7) of diffusion was interpreted to calculate the effective diffusivity, assuming a constant moisture diffusivity, infinite slab geometry, constant temperature, negligible external resistance, and uniform initial moisture distribution (Lemus-Mondaca, Zambra, Vega-Gálvez, & Moraga, 2013).

$$MR = \frac{M_t - M_e}{M_0 - M_e} = \frac{8}{\pi^2}\sum_{n=1}^{\infty}\frac{1}{(2n-1)^2}\exp\left(\frac{-(2n-1)^2\pi^2 D_{eff}\,t}{4L^2}\right) \quad (8)$$

where $D_{eff}$ is the effective diffusivity coefficient ($m^2/s$); $L$ is the thickness of the slab ($m$), and $n$ is the number of terms in Fick's equation. The first term of series solution from Equation (6) can be used for long times of drying.

$$MR = \frac{8}{\pi^2}\exp\left(\frac{-\pi^2 D_{eff}\,t}{4L^2}\right) \quad (9)$$

## 2.5 | Determination of film quality properties

Before characterization, all the films were maintained for 24 hr in desiccators. Figure 1 shows the final appearance of the dried films before characterization.

### 2.5.1 | Water activity ($a_w$) and thickness measurement

Water activity ($a_w$) was measured by a water activity meter at 25°C (AquaLab, 4TE). All $a_w$ measurements were performed in triplicate.

The thickness of film samples was measured using a micrometer (MDC-25M, Mitutoyo), with 0.01 mm resolution. Thickness was measured in 15 samples, with six measurements at different points in each one.

### 2.5.2 | Mechanical analysis

Vinasse films were cut into strips of 30 × 15 mm for tensile strength (TS) test by a texture analyzer (TA-XT2i, Stable Micro Systems Ltd.). This test was performed at room temperature with an initial grip spacing of 10 mm and cross-head speed of 0.5 mm/s (21.0°C ± 1.5°C). The TS was obtained as follows:

$$\text{Tensile strain (TS)} = \frac{\text{(Maximum force at break)}}{\text{(Initial cross}-\text{sectional area of the film)}}\left(\frac{N}{m^2}\right) \quad (10)$$

The elongation at break was calculated as the relative increase in length:

$$\text{Elongation at Break (EB)} = \frac{L_f - L_0}{L_0}\times 100\,(\%) \quad (11)$$

Young's Modulus (YM) was calculated from the initial slope of the stress–strain curve using the Texture Expert version.

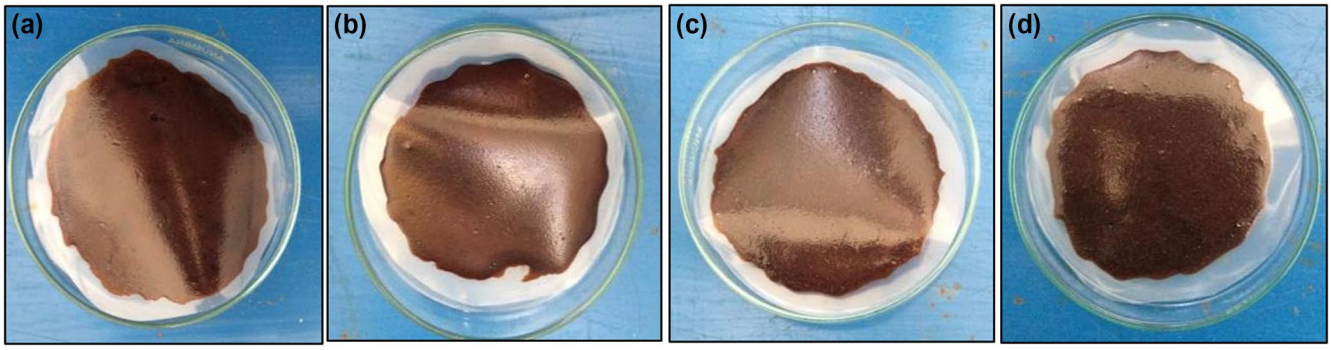


**FIGURE 1** Images of Vinasse films: (a) G-C-M-7 at 60°C, (b) G-C-M-7 at 80°C, (c) G-C-M-11 at 60°C, and (d) G-C-M-11 at 80°C. *G, Glycerol; C, Collagen; M, Maltodextrin; 7, pH 7; 11, pH 11

### 2.5.3 | Chemical characterization by Attenuated Total Reflectance-Fourier Transform Infrared Spectroscopy (ATR-FTIR)

ATR-FTIR spectra of vinasse films were obtained by PerkinElmer Spectrum Two™ with Universal Attenuated Total Reflectance (UATR) accessory of the spectrometer to study the functional groups. The measuring probe directly touched the surface of the films. A spectral resolution of 4/cm was employed and 32 scans were acquired for each spectrum in the wavelengths range of 4000–500/cm. Three samples from each experimental condition were used for each spectra measurement. The resultant film-averaged spectrum was smoothed with a fifteen-point under adaptive-smoothing function to remove the possible noises, and then, baseline modification and normalized function were applied.

### 2.6 | Statistical analysis

The drying process effect on film quality properties was estimated by analysis de variance (ANOVA) with Statgraphics Centurion software XVI, 16.1.03 version (StatPoint Inc.). Differences among the media were analyzed using the least significant difference test with a significance level of $\alpha = .05$ and a confidence interval of 95% ($p < .05$). Also, the multiple range test (MRT) included in the statistical program was used to demonstrate the existence of homogeneous groups within each of the properties.

## 3 | RESULTS AND DISCUSSION

### 3.1 | Vinasse composition

The proximate analysis of vinasse presented an initial moisture content of 97.32 g/100 g, crude protein (N × 6.25) of 0.40 g/100 g, crude ash of 0.40 g/100 g, total lipids 0.18 g/100 g and available carbohydrates (by difference) of 1.70 g/100 g. It should be noted, that the initial water content value of the vinasse is pretty high compared to those agro-industrial wastes reported by Alburquerque, Gonzálvez, García, and Cegarra (2004) in olive-cake waste (65%) and Uribe et al. (2013) in olive-cake waste (65.4%).

### 3.2 | Drying kinetics of vinasse films

As for the drying process for obtaining vinasse films were performed at 60°C and 80°C. The moisture ratio is a dimensionless parameter to normalize the drying curves that was calculated by the dry basis moisture content from vinasse films. Figure 2 shows the moisture ratio versus drying time for the experimental moisture content at different conditions and the curve fitting with the drying time for three drying models was calculated (Weibull, Page, and Modified Page models). The curves for experimental and predicted data showed an evident exponential tendency and as the drying temperature increased, moisture ratio (MR) decreased for all vinasse films. Likewise, in Figure 2 was observed

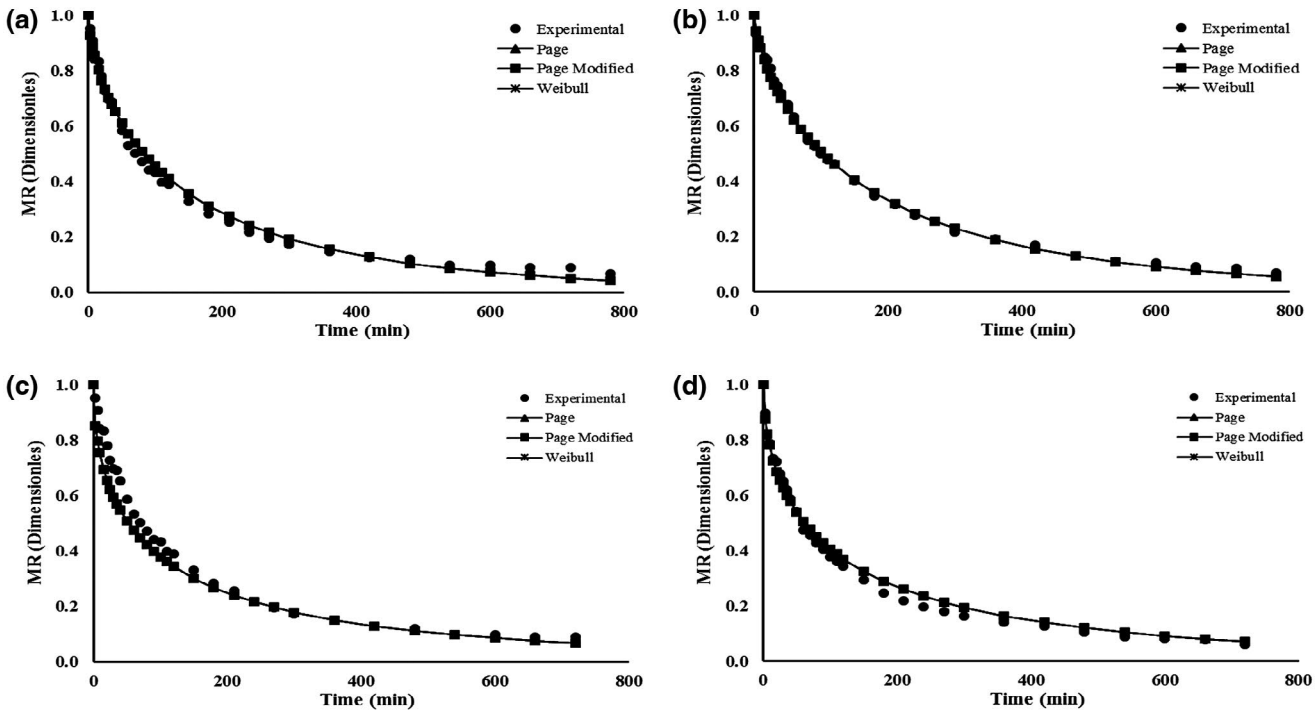


**FIGURE 2** Drying kinetics and modeling of Vinasse films: (a) G-C-M-7 at 60°C, (b) G-C-M-11 at 60°C, (c) G-C-M-7 at 80°C, and (d) G-C-M-11 at 80°C. *G, Glycerol; C, Collagen; M, Maltodextrin; 7, pH 7; 11, pH 11

that the drying time decreased as drying temperature increased to obtain similar final moisture content. Adhikari, Chaudhary, and Clerfeuille (2010); Moreira et al. (2011); Zhou et al. (2018), and Forţu, Negoescu, and Mămăligă (2019) presented similar drying curves behavior for different kinds of biofilms obtained from low-amylose starch, chestnut starch, carrageenan, pullulan, alginate, blend, polyvinyl and cellulose acetate–tetrahydrofuran films under range temperatures between 30°C and 60°C using hot-air oven drying method.

To evaluate the kinetics of the drying process from foods allows to reduce the unfavorable factors, such as temperature, water diffusion rate through the product, load density, thickness and shape of the product. An appropriate design of the drying process allows to obtain high-quality dried products (Zura-Bravo et al., 2019). Table 2 shows the kinetic parameters ($k$, $n$, $\alpha$, and $\beta$) at 60°C and 80°C, obtained from Page, modified Page and the Weibull models. In Page and Modified Page models, the parameter $k$ is the drying constant (Darvishi, Azadbakht, Rezaeiasl, & Farhang, 2012). The parameters $k$ significantly ($p < .05$) increased as the drying temperature increased. The $n$ constants are recognized as empirical parameters that could depend on the presence of an external coating (e.g., skin in fruits) (Ah-Hen, Zambra, Aguëro, Vega-Gálvez, & Lemus-Mondaca, 2013). This constant showed that there was statistically significant difference and thus dependence on the drying temperature for Page and Modified Page models. For the Weibull model, ANOVA analysis showed that the $\alpha$ decreased ($p < .05$) with an increase in the drying temperature. The mass transfer rate at the beginning of the drying process is related to the shape parameter ($\alpha$), since a low value of $\beta$ indicates that the drying rate is faster at the beginning of the process (Aghbashlo, Kianmehr, & Arabhosseini, 2010). ANOVA analysis showed that the $\beta$ decreased ($p < .05$) with increasing in drying temperature. This scale parameter determines the rate and represents the sample position required to obtain about 29.89% of the process (Aghbashlo et al., 2010). Therefore, the mass transfer rate at the beginning was slower in the drying process. This trend was observed by Aghbashlo et al. (2010) for apple slices, where an increase in the drying temperature showed a decrease in $\alpha$ and $\beta$ values.

The $\chi^2$ and *SSE* tests were evaluated to support the reliability of the Page, Modified Page, and Weibull models. A good fit is said to occur between experimental and predicted values of the models when $\chi^2$ and *SSE* are low. The best curve fitting calculations were obtained for the Weibull model. The $\chi^2$ from $1.75 \times 10^{-7}$ to $1.42 \times 10^{-10}$ and *SSE* from 0.0001 to 0.0002 for all films. Zhou et al. (2018) also found that the Midilli–Kucuk model predicted better the drying kinetics of their developed films within the temperature range studied. The Page and modified Page models also showed considerably low values for $\chi^2$ from $3.99 \times 10^{-5}$ to $1.20 \times 10^{-8}$ and *SSE* from 0.0001 to 0.0006 for all films studied. These tests indicated a good fit to the experimental data. In addition, the $R^2$ values for all samples of the Page, Modified Page and Weibull models were all above .95.

**TABLE 2** Kinetics and empirical parameters of three thin-layer drying models used for the vinasse films drying curves at 60 and 80°C, respectively

| Vinasse film | Drying Temperature (°C) | Empirical model | | | | | | |
|---|---|---|---|---|---|---|---|---|
| | | Page | | Page Modified | | Weibull | | |
| | | $n$ | $k$ | $n$ | $k$ | $\alpha$ | $\beta$ |
| G-C-M-7 | 60 | 0.6733 ± 0.0446$^a$ | 0.0361 ± 0.0098$^a$ | 0.6733 ± 0.0446$^a$ | 0.0070 ± 0.0006$^a$ | .6733 ± .0446$^a$ | 143.77 ± 12.39$^a$ |
| G-C-M-11 | | 0.7067 ± 0.0077$^a$ | 0.0264 ± 0.0033$^a$ | 0.7067 ± 0.0077$^a$ | 0.0058 ± 0.0009$^a$ | .7067 ± .0077$^a$ | 173.84 ± 24.28$^c$ |
| G-C-M-7 | 80 | 0.5992 ± 0.0135$^b$ | 0.0889 ± 0.0065$^b$ | 0.5992 ± 0.0135$^b$ | 0.0094 ± 0.0003$^b$ | .5992 ± .0135$^b$ | 106.00 ± 3.31$^b$ |
| G-C-M-11 | | 0.5432 ± 0.0188$^b$ | 0.0743 ± 0.0084$^b$ | 0.5432 ± 0.0188$^b$ | 0.0083 ± 0.0004$^b$ | .5432 ± .0188$^b$ | 120.87 ± 6.26$^{ab}$ |

*G, Glycerol; C, Collagen; M, Maltodextrin; 7, pH 7; 11, pH 11.

### 3.3 | Effective moisture diffusivity

The key drying parameter is effective moisture diffusivity ($D_{eff}$) because represents the conductive term of all moisture transfer mechanisms (Chen, Zheng, & Zhu, 2012). Table 3 shows the effective moisture diffusivity ($\times 10^{-11}$) during the drying of vinasse films at 60°C and 80°C derived by Equation 9. The lowest value of effective moisture diffusivity was $2.234 \times 10^{-11}$ $m^2/s$ at 60°C for the G-C-M-11 film. However, there were no statistically significant differences between G-C-M-7 and G-C-M-11 films. The highest value of effective moisture diffusivity was $2.513 \times 10^{-11}$ $m^2/s$ at a drying temperature of 80°C for the G-C-M-11 film. However, there was no significant difference with the G-C-M-7 film at 80°C. The $D_{eff}$ increased with an increase in the drying temperature ($p < .05$).

Park and Kim (2000) found diffusion coefficient values increased from $6.7 \times 10^{-11}$ to $5.7 \times 10^{-10}$ $cm^2/s$ with temperature from 30°C to 80°C during the with Polyimide (PI) films drying. Wong, Ashikin, and Law (2014) presented $D_{eff}$ values between 1.22 and $11.57 \times 10^{-13}$ $m^2/s$ for solid films fabricated of 1–4%w/w sodium alginate solution at 40°C, 60°C, and 80°C using to hot-air oven drying. Similar variations were reported by Adhikari et al. (2010) who found $D_{eff}$ values of $9.96 \times 10^{-10}$–$9.11 \times 10^{-11}$ $m^2/s$ for xylitol-water system and $9.74 \times 10^{-10}$–$2.99 \times 10^{-11}$ $m^2/s$ for the glycerol–water system, both films dried at 60°C. In addition, Reis et al. (2013) for yam starch and glycerol filmogenic solutions which were dried under a range of 25°C and 45°C, $D_{eff}$ values reached were between $1.8 \times 10^{-11}$ and $2.0 \times 10^{-1}$ $m^2/s$.

### 3.4 | Quality properties of vinasse films

#### 3.4.1 | Moisture content

The moisture content can affect the microbiological, chemical, and physical properties of vinasse films; thus, the moisture content or water content was an important parameter to consider their use as a film. The moisture content of the vinasse films ranged between 27.0% and 31.5% (Table 4). The pH of vinasse films did not affect the moisture content at the same drying temperature. Moreover, the drying temperature affected the moisture content, because the vinasse films that were dried at 60°C presented higher moisture content than vinasse films were dried at 80°C. Drying time can explain this behavior, since the results at lower temperature have a delay drying duration. Homez-Jara et al. (2018) reported that intermolecular forces are formed during a long drying process showing a reorganization of the solution structure, obtaining a gel-net and the succeeding formation of the film. Thus, the fast water evaporation due to a higher temperature during the drying process limit gel formation. Wahyuni and Arifan (2018) reported that a tendency to decrease the moisture content of the films from chitosan with a temperature increase was obtained.

**TABLE 3** Effective moisture diffusivity during the drying of vinasse films at different temperatures

| | Effective moisture diffusivity ($\times 10^{-11}$ $m^2/s$) | |
|---|---|---|
| Vinasse film* | 60°C | 80°C |
| DW-G-C-M-7 | $2.296 \pm 0.023^{a.A}$ | $2.499 \pm 0.023^{a.B}$ |
| DW-G-C-M-11 | $2.234 \pm 0.084^{a.A}$ | $2.513 \pm 0.070^{a.B}$ |

*G, Glycerol; C, Collagen; M, Maltodextrin; 7, pH 7; 11, pH 11.

#### 3.4.2 | Water activity ($a_w$) and thickness

The water activity ($a_w$) is a relevant parameter in food because the values above 0.95 could provide sufficient moisture to support bacteria, yeasts, and mold growth (Food and Drug Administration, 1984). Therefore, a low water activity inhibits the degradation of the films. Vinasse films have presented $a_w$ values between 0.420 and 0.410 (Table 4). Therefore, a low water activity will inhibit the degradation of the films. The pH and drying temperature of vinasse films did not affect the water activity.

The thickness of the films dried at 60°C and 80°C was measured. Films dried at 80°C showed significantly lower thicknesses of 0.100 ± 0.02 mm at 60°C to 0.080 ± 0.02 mm at 80°C. The drying temperature had an inversely proportional effect on the thickness values of the vinasse films. This performance can be due to high thermal stress (80°C or higher temperatures) lead to films structure collapse and other physicochemical (water vapor and/or oxygen permeability) and mechanical properties such as the and the possibility of decreasing biological activities, for example, antimicrobial (Jansson & Thuvander, 2004; Thakhiew, Devahastin, & Soponronnarit, 2013). This behavior has also been observed for alginate (Bagheri et al., 2019) and chitosan films (Thakhiew et al., 2013).

#### 3.4.3 | Mechanical analysis

Durability and the ability to preserve films' integrity during manipulation, transport, and storage are important factors that can

**TABLE 4** Moisture content and water activity of vinasse films under different conditions

| Temperature (°C) | Vinasse film | Moisture content (g 100/g) | Water activity ($a_w$) |
|---|---|---|---|
| 60 | G-C-M-7 | $31.29 \pm 2.58^{a.A}$ | $0.420 \pm 0.007^{a.A}$ |
| | G-C-M-11 | $31.58 \pm 0.24^{a.A}$ | $0.415 \pm 0.003^{a.A}$ |
| 80 | G-C-M-7 | $28.63 \pm 1.06^{a.AB}$ | $0.412 \pm 0.005^{a.A}$ |
| | G-C-M-11 | $27.04 \pm 1.60^{a.B}$ | $0.410 \pm 0.003^{a.A}$ |

[a]G, Glycerol; C, Collagen; M, Maltodextrin; 7, pH 7; 11, pH 11.

be assessed by measuring mechanical properties such as tensile strength, elongation at break and Young's modulus. The obtained TS, EB, and YM values of the vinasse films are shown in Figure 3. The TS corresponds to the maximum force per area needed to break the vinasse films during traction (Liu, Cao, Ren, Wang, & Zhang, 2019). The TS values were 12.06 ± 1.03 and 16.40 ± 0.01 (MPa) for G-C-M-7, 22.07 ± 2.16 and 26.54 ± 0.66 (MPa) for G-C-M-11 at 60°C and 80°C, respectively. The TS values increased when the pH and drying temperature increased. Thus, an increase in pH and drying temperature promoted a higher interaction to the polymer bonds, significantly higher TS values ($p < .05$).

The second parameter evaluated was EB, which refers to the capacity of the films to stretch up to its rupture point (Liu et al., 2019). The EB ranges extended from 6.54% to 9.31%. The EB of vinasse films decreased significantly ($p < .05$) with increased drying temperature, from 24.21% to 26.7% for G-C-M-7 and G-C-M-11. Therefore, the drying temperature had an inversely proportional effect on the EB. During long periods of drying, the water is included in the structure of the films and operates as a plasticizer, this explains the EB values of films after the drying process (Homez-Jara et al., 2018). Moreover, the YM is defined as the capacity of a material to withstand changes in longitude during tension or compression (Kumar, Mahanty, & Chattopadhyay, 2019). Also, Jansson and Thuvander (2004) explained that the strength is reduced as thickness is decreased where the degree of molecular stretch is expected to decrease with decreasing thickness. The YM values were 139.87+ ± 11.81 and 250.90+ ± 0.14 (MPa) for G-C-M-7, 236.75 ± 9.28 and 385.32 ± 14.85 (MPa) for G-C-M-11 at 60°C and 80°C, respectively. In Figure 3 shows that the YM increased when the pH and drying temperature increased. In summary, the vinasse films dried at 80°C showed higher TS and YM and lower EB. The same behavior of the vinasse films was found for alginate films (Bagheri et al., 2019) and amaranth flour films (Tapia-Blácido, Sobral, & Menegalli, 2013). Zhang, Yu, Jiang, and Wang (2016) reported that when the moisture content increases, the YM and TS decreased; contrariwise, the EB increased in microfibrillated cellulose films. Since the films are mainly constituted by hydrogen bonds and its mechanical parameters depend on the properties of the hydrogen bond network, the water molecules can break easily. Thus, a film with high humidity will be weaker and softer.

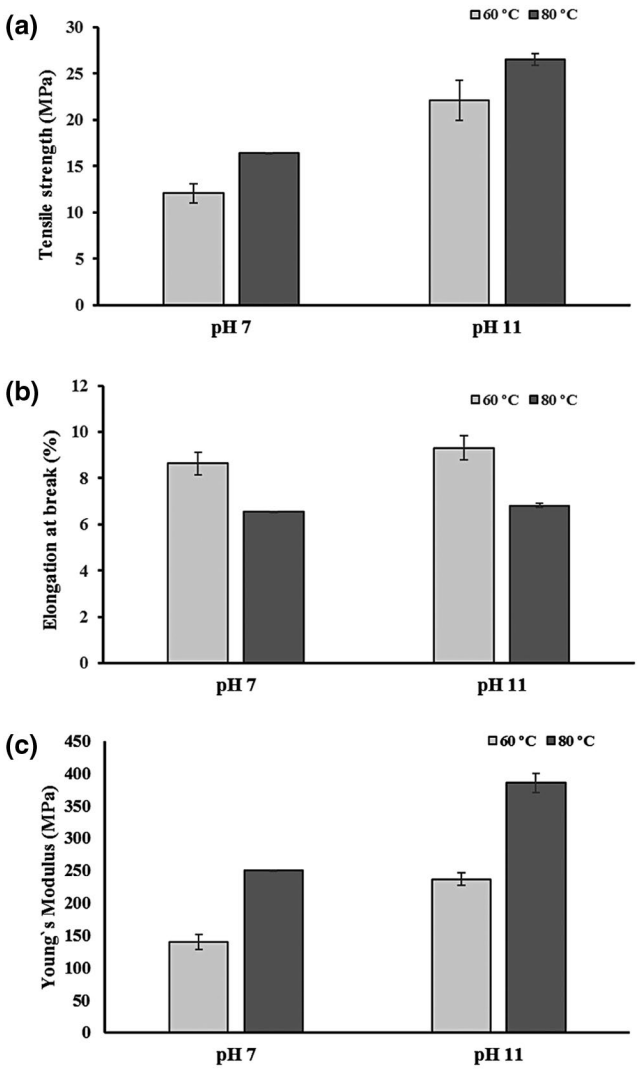


**FIGURE 3** Textural analysis of G-C-M: (a) Tensile strength (MPa) (b) elongation at break (%), and (c) Young`s modulus (MPa) of vinasse films plasticized with glycerol

### 3.4.4 | Chemical characterization by ATR-FTIR

Figure 4 shows the spectra by ATR-FTIR of vinasse films (a) G-C-M-7 and (b) G-C-M-11 at 60°C, as well as (c) G-C-M-7 and (d) DW-G-C-M-11 at 80°C. The ATR-FTIR analysis was measured to detect the functional groups present in vinasse films. In general, the Figure 4(a–d) show the same presence of functional groups in the ATR-FTIR spectra of the vinasse films at different pH and drying temperature conditions. The vinasse films showed a broadband ranging between 3,500 and 3,000/cm, assigned to the O–H and N–H stretching vibration, asymmetric and symmetric vibration of -$CH_2$ stretches were observed at peaks 2,932.50 and 2,878.68/cm, respectively. The spectra also show other peaks assigned to vibrational modes that are present in film components such as C–O stretching (amide I) at 1,600.02/cm from collagen (Belbachir, Noreen, & Gouspillou, 2014), carboxylates groups at 1,400.02/cm due to the presence of acetic acid of the pisco. Acetic acid is considered a volatile and congener component of the pisco (Hidalgo, Hatta, & Palma, 2016). Hidalgo et al. (2016) reported that there was a presence of acetic acid in pisco from wines with and without sediment. According to Ferreira, Nunes, Castro, Ferreira, and Coimbra (2014), they indicated that the C–C and C–O linkages ranging between 1,150 and 800/cm (peak 6; 1,100.02 and peak 7; 1,029.26/cm) correspond from the polysaccharide and the glycerol.

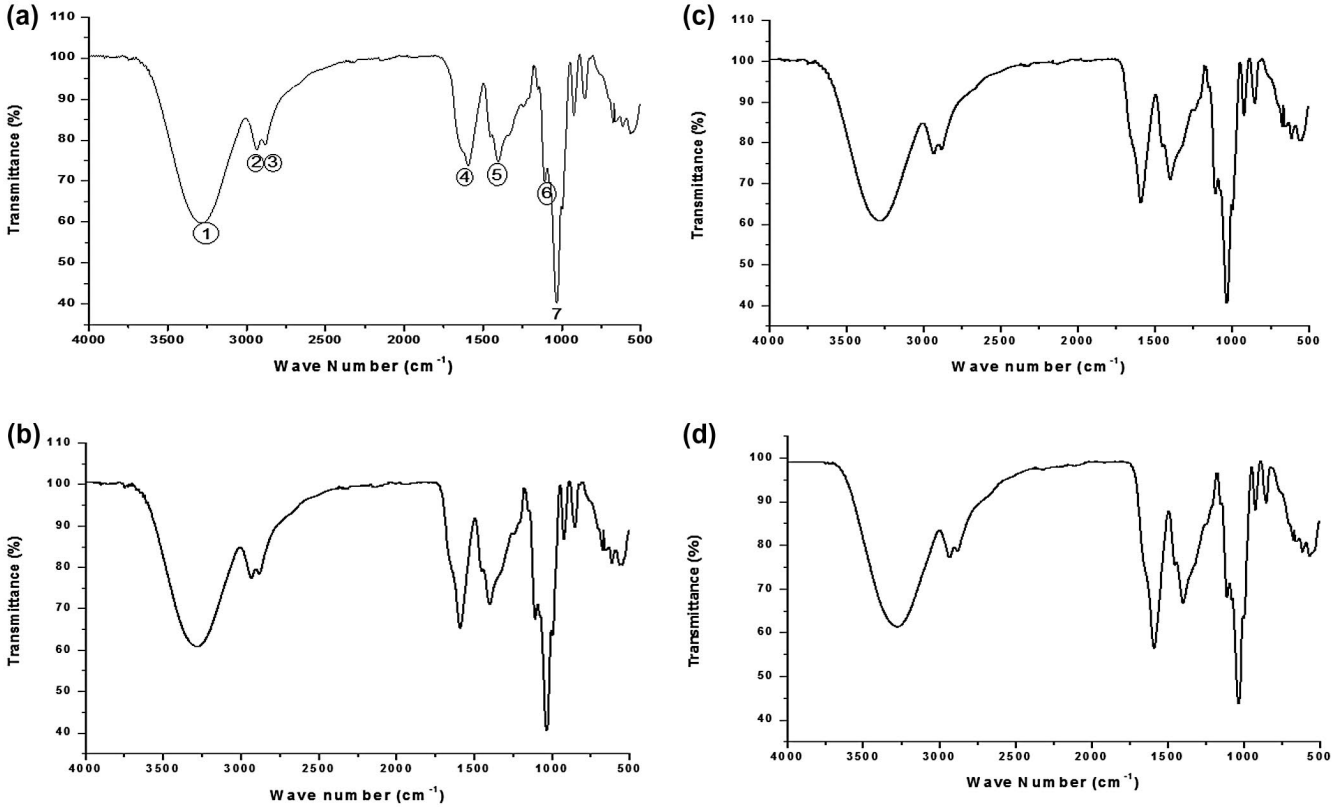


**FIGURE 4** Spectra of ATR-FTIR obtained from vinasse films: (a) G-C-M-7 at 60°C, (b) G-C-M-11 at 60°C, (c) G-C-M-7 at 80°C, and (d) G-C-M-11 at 80°C

## 4 | CONCLUSIONS

This investigation showed the preparation/obtaining of films based on vinasse and glycerol has high potential as packaging or coating material. The drying curves for experimental and predicted data showed an evident exponential tendency. The best curve fitting was obtained for the Weibull model for all different conditions of the film's preparation. The films presented a low moisture content and water activity, which would not allow the growth of microorganisms. The mechanical properties of the vinasse films dried at 80°C showed higher TS and YM and lower EB. ATR-FTIR analysis suggested the presence of functional groups from bioactive compounds. Thus, vinasse films would become interesting in the application of the food packaging. Future research is suggested on the study of the bioactive compounds release, hygroscopic properties, its application on preventing weather-induced fruit splitting, and analysis of antimicrobial activity of these films on a food surface, as well as a sensorial evaluation as to consumer acceptance or not. In consequence, converting a by-product of the pisco production into value-added films could increase revenue for wine-making industry.

## ACKNOWLEDGMENTS

This work was supported by the Departamento de Ingeniería en Alimentos, Universidad de La Serena and Project PR16331/PEQ16334 and Compañía Pisquera de Chile S.A. (CPCh), located in Ovalle city, Region of Coquimbo, Chile.

## CONFLICT OF INTEREST

The authors have declared no conflicts of interest for this article.

## ORCID

*Roberto Lemus-Mondaca* https://orcid.org/0000-0002-1252-2573
*Claudia Giovagnoli-Vicuna* https://orcid.org/0000-0001-5840-5439
*Elsa Uribe* https://orcid.org/0000-0002-7608-1180

## REFERENCES

Adhikari, B., Chaudhary, D. S., & Clerfeuille, E. (2010). Effect of plasticizers on the moisture migration behavior of low-amylose starch films during drying. *Drying Technology: An International Journal*, *28*(4), 468–480. https://doi.org/10.1080/07373931003613593

Aghbashlo, M., Kianmehr, M. H., & Arabhosseini, A. (2010). Modeling of thin-layer drying of apple slices in a semi-industrial continuous band dryer. *International Journal of Food Engineering*, *6*(4).1–15.

Ah-Hen, K., Zambra, C. E., Aguëro, J. E., Vega-Gálvez, A., & Lemus-Mondaca, R. (2013). Moisture diffusivity coefficient and convective drying modelling of murta (*Ugni molinae* Turcz): Influence of temperature and vacuum on drying kinetics. *Food and Bioprocess Technology*, *6*(4), 919–930.

Alburquerque, J. A., Gonzálvez, J., García, D., & Cegarra, J. (2004). Agrochemical characterisation of "alperujo", a solid by-product of the two-phase centrifugation method for olive oil extraction. *Bioresource Technology*, *91*, 195–200.

AOAC. (1990). *Official method of analysis*, Association of Official Analytical Chemists (15th ed.). Arlington, VA: Association of Official Analytical Chemists, Inc.

Bagheri, F., Radi, M., & Amiri, S. (2019). *Drying conditions highly influence the characteristics of glycerol-plasticized alginate films*, Vol. *90*. Elsevier Ltd.

Barba, F. J., Zhu, Z., Koubaa, M., Sant'Ana, A. S., & Orlien, V. (2016). Green alternative methods for the extraction of antioxidant bioactive compounds from winery wastes and by-products: A review. *Trends in Food Science and Technology*, *49*, 96–109.

Bekhit, A. E., Din, A., Cheng, V. J., Zhang, H., Mros, S., Mohamed, I. A., … McConnell, M.. (2019). Effect of extraction system and grape variety on anti-influenza compounds from wine production residue. *Food Control*, *99*, 180–189. https://doi.org/10.1016/j.foodcont.2018.12.036

Belbachir, K., Noreen, R., Gouspillou, G., & Petibois, C. (2014). Collagen types analysis and differentiation by FTIR spectroscopy. *Analytical and Bioanalytical Chemistry*, *395*(3), 829–837.

Botelho, R. V., Bennemann, G. D., Torres, Y. R., & Sato, A. J. (2018). Potential for use of the residues of the wine industry in human nutrition and as agricultural input. In A. M. Jordão & F. Cosme (Eds.), *Grapes and wines: Advances in production, processing, analysis and valorization* (1st ed., pp. 325–336). London, UK: InTechOpen Ltd.

Callejas, R., Silva, Á., Peppi, C., & Seguel, Ó. (2014). Factibilidad agronómica del uso de vinaza, subproducto de la fabricación del pisco, como biofertilizante en viñedos. *Revista Colombiana De Ciencias Hortícolas*, *8*(2), 230–241.

Chen, D., Zheng, Y., & Zhu, X. (2012). Determination of effective moisture diffusivity and drying kinetics for poplar sawdust by thermogravimetric analysis under isothermal condition. *Bioresource Technology*, *107*, 451–455.

Chuaynukul, K., Nagarajan, M., Prodpran, T., Benjakul, S., Songtipya, P., & Songtipya, L. (2018). Comparative characterization of bovine and fish gelatin films fabricated by compression molding and solution casting methods. *Journal of Polymers and the Environment*, *26*(3), 1239–1252.

Darvishi, H., Azadbakht, M., Rezaeiasl, A., & Farhang, A. (2012). Drying characteristics of sardine fish dried with microwave heating. *Journal of the Saudi Society of Agricultural Sciences*, *12*(2), 121–127.

Daza, L. D., Homez-Jara, A., Solanilla, J. F., & Váquiro, H. A. (2018). Effects of temperature, starch concentration, and plasticizer concentration on the physical properties of Ulluco (*Ullucus tuberosus* Caldas)-based edible films. *International Journal of Biological Macromolecules*, *120*, 1834–1845.

Ferreira, A. S., Nunes, C., Castro, A., Ferreira, P., & Coimbra, M. A. (2014). Influence of grape pomace extract incorporation on chitosan films properties. *Carbohydrate Polymers*, *113*, 490–499.

Food and Drug Administration. (1984). *Water activity (aw) in foods*. Inspections, Compliance, Enforcement, and Criminal Investigations, Inspection References, Inspection Guides, Inspection Technical Guides (Vol. 39). Maryland, USA.: Food and Drug Administration FDA. Retrieved May 9, 2019. https://www.fda.gov/inspections-compliance-enforcement-and-criminal-investigations/inspection-technical-guides/water-activity-aw-foods

Forţu, I. O., Negoescu, C., & Mămăligă, I. (2019). Effects of drying conditions on polyvinyl alcohol-water and cellulose acetate-tetrahydrofuran films. *Cellulose Chemistry and Technology*, *53*(5–6), 527–535.

Hidalgo, Y., Hatta, B., & Palma, J. C. (2016). Influencia de la presencia de borras durante el tiempo de reposo del vino base sobre algunos compuestos volátiles del pisco peruano de uva Italia. *Revista De La Sociedad Química Del Perú*, *82*(3), 280–295.

Homez-Jara, A., Daza, L. D., Aguirre, D. M., Muñoz, J. A., Solanilla, J. F., & Váquiro, H. A. (2018). Characterization of chitosan edible films obtained with various polymer concentrations and drying temperatures. *International Journal of Biological Macromolecules*, *113*, 1233–1240.

Jansson, A., & Thuvander, F. (2004). Influence of thickness on the mechanical properties for starch films. *Carbohydrate Polymers*, *56*(4), 499–503.

Kumar, P., Mahanty, M., & Chattopadhyay, A. (2019). An overview of stress-strain analysis for elasticity equations. In E. Günay, *Elasticity of materials: Basic principles and design of structures* (1st ed., pp. 1–19). London, UK: IntechOpen Limited.

Lemus-Mondaca, R. A., Zambra, C. E., Vega-Gálvez, A., & Moraga, N. O. (2013). Coupled 3D heat and mass transfer model for numerical analysis of drying process in papaya slices. *Journal of Food Engineering*, *116*(1), 109–117.

Liu, Z., Cao, X., Ren, S., Wang, J., & Zhang, H. (2019). Physicochemical characterization of a zein prepared using a novel aqueous extraction technology and tensile properties of the zein film. *Industrial Crops and Products*, *130*, 57–62. https://doi.org/10.1016/j.indcrop.2018.12.071

Moreira, R., Chenlo, F., Torres, M. D., Silva, C., Prieto, D. M., Sousa, A. M. M., … Gonçalves, M. P. (2011). Drying kinetics of biofilms obtained from chestnut starch and carrageenan with and without glycerol. *Drying Technology: An International Journal*, *29*(9), 1058–1065.

Park, K. S., & Kim, D. (2000). Determination of diffusion and mass transfer coefficients during drying of solvent-absorbed polymer films. *Polymer Journal*, *32*(5), 415–421.

Reis, R. C., Côrrea, P. C., Devilla, I. A., Santos, E. S., Ascheri, D. P. R., Servulo, A. C. O., & Souza, A. B. M. (2013). Drying of yam starch (*Discorea* ssp.) and glycerol filmogenic solutions at different temperatures. *LWT - Food Science and Technology*, *50*(2), 651–656. https://doi.org/10.1016/j.lwt.2012.07.033

Tapia-Blácido, D. R., Sobral, P. J. D. A., & Menegalli, F. C. (2013). Effect of drying conditions and plasticizer type on some physical and mechanical properties of amaranth flour films. *LWT - Food Science and Technology*, *50*(2), 392–400. https://doi.org/10.1016/j.lwt.2012.09.008

Teixeira, A., Baenas, N., Dominguez-Perles, R., Barros, A., Rosa, E., Moreno, D. A., & Garcia-Viguera, C. (2014). Natural bioactive compounds from winery by-products as health promoters: A review. *International Journal of Molecular Sciences*, *15*(9), 15638–15678. https://doi.org/10.3390/ijms150915638

Thakhiew, W., Devahastin, S., & Soponronnarit, S. (2013). Physical and mechanical properties of chitosan films as affected by drying methods and addition of antimicrobial agent. *Journal of Food Engineering*, *119*(1), 140–149. https://doi.org/10.1016/j.jfoodeng.2013.05.020

Uribe, E., Lemus-Mondaca, R., Vega-Gálvez, A., López, J., Ah-Hen, K., & Di Scala, K. (2013). Quality characterization of olive-waste cake during hot air drying: Nutritional aspects and antioxidant activity. *Food and Bioprocess Technology*, *6*(5), 1207–1217.

Wahyuni, E. S., & Arifan, F. (2018). Optimization of chitosan drying temperature on the quality and quantity of edible film. *E3S Web of Conferences*, *3*, 1–5. https://doi.org/10.1051/e3sconf/20183103012

Wong, T. W., Ashikin, W. H. N. S., & Law, C. L. (2014). Evaporation and diffusion transport properties and mechanical properties of alginate dried film. *Drying Technology*, *32*(1), 117–125. https://doi.org/10.1080/07373937.2013.821479

Zhang, X., Yu, Y., Jiang, Z., & Wang, H. (2016). Influence of thickness and moisture content on the mechanical properties of microfibrillated cellulose (MFC) films. *Wood Research*, *61*(6), 851–860.

Zhou, Y., Huang, M., Deng, F., & Xiao, Q. (2018). Effect of temperature on drying characteristics of pullulan-alginate based edible films. *Food Science and Technology Research*, *24*(1), 55–62. https://doi.org/10.3136/fstr.24.55

Zura-Bravo, L., Rodriguez, A., Stucken, K., & Vega-Gálvez, A. (2019). Drying kinetics of probiotic-impregnated murta (*Ugni molinae* T.) berries. *Journal Fo Food Science and Technology*, *56*(1), 103–113. https://doi.org/10.1007/s13197-018-3463-9

**How to cite this article:** Cortes L, Pérez-Won M, Lemus-Mondaca R, Giovagnoli-Vicuna C, Uribe E. Quality properties and mathematical modeling of vinasse films obtained under different conditions. *J Food Process Preserv*. 2020;00:e14477. https://doi.org/10.1111/jfpp.14477